# A synchrotron X-ray study of competing undulation and electrostatic interlayer interactions in fluid multimembrane lyotropic phases

D. Roux, C.R. Safinya

*J. Phys. France* **49** (1988) 307-318 FÉVRIER **1988,** PAGE 307

Classification
*Physics Abstracts*
61.30E — 82.70K

# A synchrotron X-ray study of competing undulation and electrostatic interlayer interactions in fluid multimembrane lyotropic phases

D. Roux ([2, *]) and C. R. Safinya ([1])

([1]) Exxon Research and Engineering Co., Annandale, NJ 08801, U.S.A.
([2]) UCLA Chemistry department, Los Angeles, CA 90024, U.S.A.

(*Reçu le 15 juillet 1987, accepté le 14 septembre 1987*)

**Résumé.** — Il a récemment été mis en évidence, en utilisant une méthode de diffraction des rayons X, le rôle prédominant des interactions d'ondulation lors de la dilution par du dodécane d'une phase lamellaire d'un mélange quaternaire lyotrope [1]. Afin d'étudier la compétition entre les interactions d'ondulation et les forces électrostatiques, nous avons étudié l'effet de la dilution avec, soit de l'eau, soit de la saumure ($\approx 0{,}5$ mole.$l^{-1}$ NaCl), sur les interactions d'une phase lamellaire $L_\alpha$. Dans ces deux cas, la membrane chargée négativement est composée de Dodecyl Sulfate de Sodium (SDS) et de pentanol. Un montage de rayons X haute résolution, nous permet de mesurer, en fonction de la distance de séparation entre membranes ($d$), l'exposant $\eta(d)$ qui caractérise la loi de puissance du facteur de structure obtenue en rayons X. Cet exposant $\eta$ est directement relié aux interactions entre membranes. Nous avons établi que les interactions électrostatiques à longue portée dominent lors de la dilution par de l'eau. Lors de la dilution par de la saumure, l'adjonction de sel réduit la longueur de Debye ($\lambda_D/d \ll 1$). Dans ce cas où les interactions électrostatiques sont à courte portée, les interactions d'ondulation dominent de nouveau avec $\eta(d) = 1{,}33(1 - \delta/d)^2$ ($\delta$ est l'épaisseur de la membrane), fonction qui sature à une valeur constante à large distance $d$ conformément aux prédictions de la théorie d'Helfrich [4].

**Abstract.** — Recent X-ray work [1] in a quaternary lyotropic lamellar phase demonstrated that entropically induced undulation forces dominated the free energy of interaction between fluid membranes swollen by dodecane. Here we report on a comprehensive X-ray study of competing electrostatic and undulation forces in two multimembrane systems in the lamellar $L_\alpha$ phase as a function of the intermembrane distance. In each case, the negatively charged membrane is composed of a mixture of Sodium Dodecyl Sulfate (SDS) and pentanol, while the solvent separating the membranes is either pure water or brine ($\approx 0.5$ mole.$l^{-1}$ of NaCl). A specialized high resolution X-ray spectrometer enables us to measure, as a function of the intermembrane distance ($d$), the exponent $\eta(d)$ which characterizes the algebraic decay of layer correlations. In turn, $\eta(d)$ is directly related to the intermembrane interactions. The results clearly show that when diluting with pure water the interactions are dominated by long range electrostatic forces. In the brine dilution system, the addition of free ions (NaCl) to the solvent yields a small Debye length ($\lambda_D/d \ll 1$). In this case, with short range electrostatic interactions, undulation forces are restored with $\eta(d) = 1.33(1 - \delta/d)^2$ ($\delta$ is the membrane thickness) approaching a constant value for large $d$, as predicted by Helfrich [4].

## 1. Introduction.

The understanding of interactions between membranes, has attracted a lot of attention in the last decade because of their relevance in biological processes such as cell-cell contact. The fundamental interactions between membranes arise from attractive electrodynamic van der Waals and, normally repulsive electrostatic forces [2]. On a more empirical level, Parsegian *et al.* and Rand [3, 10] have shown that at very small intermembrane distances an extremely strong repulsive potential acts to prevent the approach of phospholipid bilayers embedded in water. This repulsive interaction, which decays exponentially with a typical length of a few angtroms, is attributed to the hydration of the phospholipid head groups and dominates for distances less than 20 Å.

More recently, Helfrich [4] has proposed that thermally induced out of plane fluctuations of memb-

(*) *Permanent address :* CRPP CNRS and Greco « Microemulsions », Domaine Universitaire, 33405 Talence Cedex, France.

ranes in a multilayer system can lead to an effective long range repulsive force. This undulation interaction arises from the difference in entropy between a fluctuating « free » membrane and a « bound » membrane in a multilayer system. The crucial elastic modulus which controls the strength of this interaction is $k_c$ associated with the bending energy of a single membrane. For this steric interaction to compete with the microscopic forces ; that is, van der Waals and short range electrostatics, $k_c$ has to be of order $k_B T$ simply because it is induced by thermal fluctuations. Using renormalization group techniques R. Lipowsky and S. Leibler [5] have in fact demonstrated that in the very strong fluctuating regime, this effective long range repulsive force may lead to a complete unbinding of membranes. More generally, the dominant contribution to the free energy of a polymer confined between walls [6] or that associated with wandering walls of incommensurate phases [7] are similarly entropic in origin.

In a previous letter [1], we reported on a high resolution X-ray scattering study in the multi-lamellar phase of the quaternary system of water, dodecane, SDS and pentanol. The X-ray structure factor was measured as a function of the intermembrane distance $d$ along a dodecane dilution path. In contrast to the usual lyotropic lamellar phases where $d \approx \delta$ (membrane thickness), these recently discovered lamellar phases are systems which are stable over an extremely large dilution range leading to $d/\delta \gg 1$. These phases then constitute novel model one dimensional colloidal smectics. As we discuss below, because layered microemulsions have lower marginal dimension 3, the structure factor exhibits power law behaviour (instead of the usual delta function Bragg scattering) with a characteristic exponent $\eta(d) \propto 1/\sqrt{BK}$ where $K(d)$ and $B(d)$ are the bulk moduli for layer curvature and layer compression. Aside from subtle length scale renormalization effects of the curvature elasticity [8], we expect $K = k_c n = k_c/d$ where $n$ is the number of layers per unit height. On the other hand, the compressional modulus $B$ is *directly* related to the free energy of interaction between neighbouring membranes. Therefore, the dependence of the intermembrane forces on the distance $d$ is straightforwardly related to the power law exponent $\eta(d)$ measured in our X-ray scattering experiments. In earlier work [1], we found that as a function of $d$ along a dodecane dilution path, $\eta(d)$ was accurately predicted by the Helfrich theory which describes the free energy of interaction of undulating multilayer membranes [4]. Similar experiments [9] done on freely suspended lipid films of DMPC (dymyrystoyl-phosphatidyl choline) and water in the $L_\alpha$ phase, have shown that in this latter membrane system, spanning the accessible distances ($5\ \text{Å} < d < 15\ \text{Å}$), hydration forces are dominant. This last result is in accordance with earlier work on model membrane systems [10]. Thus, the quaternary lyotropic system studied is an example where entropically driven forces dominate. The undulation force is also expected to be important in other similar [11-13] systems. Our work leads us to conclude that the undulation forces dominate when two criteria are satisfied. First, the presence of cosurfactant molecules in addition to the surfactants in membrane films appears to be crucial. The cosurfactant is thought to significantly decrease the bending constant $k_c$ [14] of films and therefore to enhance undulation forces. Second, we require the absence of long range repulsive electrostatic forces which, as we will demonstrate, will normally completely overwhelm and suppress undulation induced forces.

In this paper we report results on the competition between electrostatic and undulation forces. We present data along two dilution paths. In each case, the negatively charged membrane is composed of a mixture of Sodium Dodecyl Sulfate (SDS) and pentanol, while the solvent separating the membranes is either pure water or brine ($\approx 0.5$ mole.$l^{-1}$ of NaCl). Both systems are similar to what was previously studied [1] but with no dodecane. We have used a high resolution synchrotron X-ray set up in order to measure the exponent $\eta(d)$ associated with the algebraic decay of layer correlations ; this in turn, allows for a direct measurement of intermembrane forces.

The outline of the paper is as follows. In part 2 we discuss the scattering spectrometer used in our work. Part 3 is a brief review of the theoretical predictions for intermembrane forces. Part 4 is a description of the samples and the phase diagrams of the different systems studied. In part 5 we present the X-ray scattering results and analysis. Parts 6 and 7 are devoted to the interpretation of the data and conclusion.

## 2. Experimental technique.

X-ray measurements normally give information on the structure of the system studied. In special cases however, such as the smectic-A phase of liquid crystals or two dimensional solids, thermodynamic properties can be obtained reliably from the analysis. It has been known for a long time that the lower marginal dimension for crystalline solids is two [15]. For an ordinary one dimensional system, long range translational order cannot exist at a temperature different from zero, since thermal fluctuations diverge with the size of the sample and thus destroy the ordering. For dimensions larger than two, solid structures are stable and fluctuations have, far from a phase transition, only a weak effect. Exactly at dimension two the situation is named marginal : in this case the fluctuations diverge as the logarithm of

the sample size. However, because this divergence is only logarithmic, the structure factor may in fact still be singular. For two dimensional solids, the normally observed Bragg peaks of the structure factor are replaced by power-law singularities [16] which signal the lack of true long range order.

An analogous analysis regarding the stability of the lyotropic-$L_\alpha$ multimembrane phase and the thermotropic smectic-A phase may be considered in three dimensions. In both cases, the Landau-de-Gennes [16] elastic free energy density may be written as

$$\frac{F}{V} = 1/2\left\{B\left[\frac{\partial u}{\partial z}\right]^2 + K\left[\left[\frac{\partial^2 u}{\partial x^2}\right] + \left[\frac{\partial^2 u}{\partial y^2}\right]\right]^2\right\} \quad (1)$$

where $u(r)$ is the layer displacement in the $z$-direction normal to the layers, and $B$ and $K$ are bulk moduli for layer compression (erg/cm$^3$) and layer curvature (erg/cm). Peierls and Landau [15] first recognized that this free energy is analogous to that used to describe a two dimensional elastic solid. Therefore, for the lyotropic $L_\alpha$ and the smectic-A liquid crystal phases, the marginal dimension is 3 and a behaviour similar to a regular crystal in two dimensions is expected [17]. The expected structure factor has been calculated by Caillé [18] based on the elastic free energy (Eq. (1)) for the smectic-A phase. The asymptotic behaviour of the structure factor in the directions parallel (//) and perpendicular ($\perp$) to the layer normal is given by simple power laws

$$S(0, 0, q_\parallel) \propto \frac{1}{|q_\parallel - q_m|^{2-\eta_m}} \quad (2a)$$

$$S(q_\perp, 0, q_m) \propto \frac{1}{q_\perp^{4-2\eta_m}} \quad (2b)$$

where $q_m$ is the position of the $m$-th harmonic of the structure factor ($q_m = mq_0$, $m = 1, 2, \ldots$) and $\eta_m$ is the power law exponent related to the elastic constants $B$ and $K$:

$$\eta_m = m^2 q_0^2 \frac{kT}{8\pi\sqrt{BK}}. \quad (3)$$

A previous study [19] of the structure factor for the first harmonic of a smectic-A phase is consistent with the power law description of $S(0, 0, q_\parallel)$. Our recent work [1] in a quaternary lyotropic lamellar phase has confirmed the power law behaviour and the scalling of $\eta_m$ with $m^2$ for the first and the second harmonics of $S(q)$. The expressions given by (2a) and (2b) are simple but the asymptotic behaviour of the structure factor does not yield all the physical information obtainable from the data. Indeed, the structure factor is given by the Fourier transform of the correlation function [18, 19]

$$G(\mathbf{R}) = G(\rho, z) \propto \left[\frac{1}{\rho}\right]^{2\eta} e^{-\eta\left[2\gamma + E_1\left(\frac{\rho^2}{4\lambda z}\right)\right]}. \quad (4)$$

Here, $\gamma$ is Euler's constant, $E_1(x)$ is the exponential integral function, $R^2 = z^2 + \rho^2$, with $\rho^2 = x^2 + y^2$, $\eta$ has been defined previously (equation (3)) and $\lambda$ is a length related to the elastic constants ($\lambda = \sqrt{K/B}$). It is the limiting behaviour of the Fourier transform of this correlation function for $q_\parallel = 0$ and $q_\perp = 0$ which gives the simple expressions of equation (2). When these two limiting behaviours are calculated, the function $G(\rho, z)$ is independent of $\lambda$, but in general it does depend on both parameters $\eta$ and $\lambda$. However, we will see that the fit of the experimental data is sensitive to $\lambda$ only when $\lambda \leqslant 2\pi/q_0$.

We have seen how we can, in principle, extract the elastic constants of a smectic A liquid crystal from the X-ray structure factor. To unambiguously study the line shape of the structure factor one must use a specialized spectrometer. In fact, the experimental set-up must have a very high resolving power capable of determining length scales on the order of a micron to probe the interesting long wave length behaviour of the system. In addition, the tail of the resolution function must decrease as a function of the wave vector $q$ faster than $1/q^2$ which is the fall off expected for the structure factor of a « Landau-Peierls » system with a small value of $\eta$. These two requirements are fulfilled when using the high resolution spectrometer [19, 20] shown in figure 1. The experiments were carried out at the National Synchrotron light Source on the Exxon Beam line X-10A. The monochromator (Fig. 1) consists of a double bounce Si(1, 1, 1) crystal. The analyser is a triple bounce Si(1, 1, 1) channel cut crystal. The configuration yields a very sharp in-plane Gaussian resolution function with very weak tail scattering with Half Width at Half Maximum (*HWHM*) $8 \times 10^{-5}$ Å$^{-1}$. This then enables us to resolve length scales as large as 1.5 μm. The channel cut crystals cut down the tails of the resolution function ; indeed it is known [19, 20] that after $m$ reflections from a perfect crystal the resolution is given by the resolution of a single reflection to the $m$-th power. In our case, since the tail intensity fall off is limited by the monochromator double bounce we have checked that the tails decrease approximatively as $1/q^4$. The out-of-plane resolution was set by narrow slits which yielded an out-of-plane gaussian resolution function with *HWHM* = 1/1 000 Å$^{-1}$.

### 3. Interaction forces.

For a system of flat membranes of thickness $\delta$ separated by a distance $d$ (the repeat distance for the lattice is $d_u = d + \delta$), the total interaction free

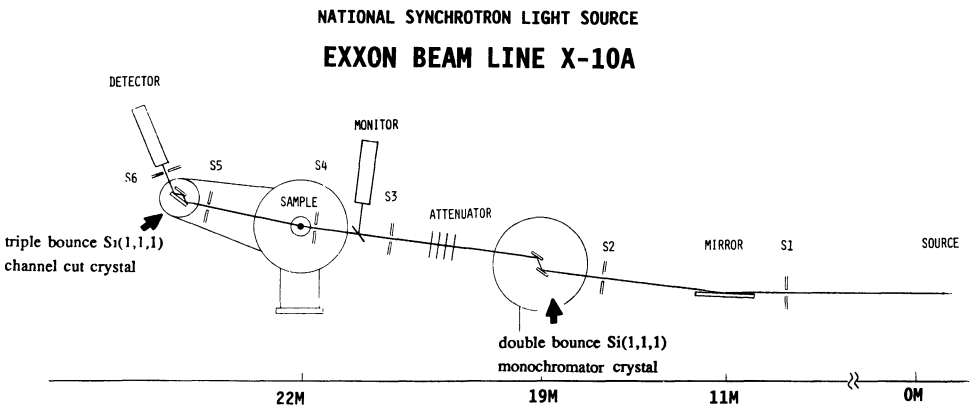


Fig. 1. — Schematic drawing of the high resolution X-ray set-up used in this study. The crucial high resolution elements are the double-bounce Si(1, 1, 1) monochromator crystal and the triple-bounce Si(1, 1, 1) analyser crystal as discussed in the text.

energy per unit surface, in the absence of layer undulations, is given by the sum of three terms :

$$f = f_{\mathrm{vdW}} + f_{\mathrm{elec}} + f_{\mathrm{hyd}} \cdot \tag{5}$$

The van der Waals force is given by a simple expression if retardation effects are neglected [21] :

$$f_{\mathrm{vdW}} = -\frac{A}{12\,\pi}\left[\frac{1}{d^2} + \frac{1}{(d+2\,\delta)^2} - \frac{2}{(d+\delta)^2}\right] \tag{6}$$

this interaction is attractive varying as $1/d^2$ for small $d$ with a crossover to $1/d^4$ for large $d$. In the retarded regime for $d > 1\,000$ Å, the van der Waals forces are weaker and vary for large distances as $1/d^5$. $A$ is the Hamaker constant and there is theoretical [21] and experimental [22] agreement on its value ($A \approx k_{\mathrm{B}}\,T$).

The hydration energy per unit surface has been measured to decay exponentially [10] ; this may be represented empirically as :

$$f_{\mathrm{hyd}} = H_0\,\mathrm{e}^{-d/\lambda_h} \tag{7}$$

where $\lambda_h$ is a microscopic length (typically 2 Å) and $H_0$ is a constant of the order of $2 \times 10^3$ erg. cm$^{-2}$ ($\approx 4\,k_{\mathrm{B}}\,T$ . Å$^{-2}$ at room temperature). This interaction dominates for distances less than 10 Å but is negligible for distances larger than 30 Å.

The electrostatic interaction can be calculated from the Poisson-Boltzmann [23] equation. If $\Psi(x)$ is the potential and $\rho(x)$ the charge density ($x$ is the distance from the charged plane), the Poisson equation reads in one-dimension :

$$\frac{\mathrm{d}^2\Psi}{\mathrm{d}x^2} = -\frac{4\,\pi\rho(x)}{\varepsilon} \tag{8}$$

depending on the boundary conditions the interaction energy per unit surface can be calculated. Two limiting cases yield simple solutions for $\Psi$. In one limit, the system consists of two uniformly (e.g. negatively) charged planes separated by the counterions (+ ) in water. The electrostatic pressure exerted on a membrane has been calculated by Cowley *et al.* [23]. In fact, recent rigorous calculations by S. Leibler and R. Lipowsky [24] indicate that the mean field treatment of electrostatic interactions [23] is valid leading to :

$$P_{\mathrm{elec}} = kT\,\frac{2\,\alpha q}{\Sigma d_{\mathrm{w}}\,\mathrm{Tan}\,(q)} \tag{9}$$

where,

$$q\,\mathrm{Tan}\,(q) = \frac{\pi\,\mathrm{e}^2\,\alpha}{\varepsilon \Sigma kT}\,d \equiv L_{\mathrm{e}}\,\frac{\alpha}{\Sigma}\,d\,. \tag{10}$$

Here, $L_{\mathrm{e}}$ as defined in equation (10) has units of length ($L_{\mathrm{e}} = 22$ Å for $\varepsilon = 80$ and $kT$ at room temperature), $\alpha$ is the dissociation coefficient (if all the charges are dissociated $\alpha = 1$, otherwise $\alpha < 1$) and $\Sigma$ is the surface area per (charged) polar head. This equation can be simplified in the approximation of high density of charges and large distances and reads :

$$P_{\mathrm{elec}} \approx \frac{\pi^2 kT}{2\,L_{\mathrm{e}}}\,\frac{1}{d^2}\left[1 + \frac{\Sigma}{\alpha d L_{\mathrm{e}}}\right]^{-2}. \tag{11}$$

The energy per unit surface is then given by

$$f_{\mathrm{elec}} = -\frac{1}{2\,S}\int_v P\,\delta v = -\frac{1}{2}\int_\infty^d P\,\delta d$$

with $S$ the area of a plate and $\delta v = S\,\delta d$

$$f_{\mathrm{elec}} = -1/2\int_\infty^d P\,\delta(d) = \frac{\pi^2 kT}{L_{\mathrm{e}}\,4\,d} \times$$

$$\times\left[1 - \frac{\Sigma}{\alpha L_{\mathrm{e}}\,d} + \left[\frac{\Sigma}{\alpha L_{\mathrm{e}}\,d}\right]^2 + \cdots\right]. \tag{12}$$

Thus, the dominant term due to this long range force varies as $1/d$. For sufficiently large additions

of ions plus counterions, such as in a NaCl solution, the Debye screening length $\lambda_D$ is now smaller than the interlayer spacing $d$ and the free energy per unit surface decays exponentially with $d$ [2] :

$$f_{elec} = E_0 \, e^{-d/\lambda_D} . \quad (13)$$

Here, $\lambda_D$(in Å) = 3.04/[$c$], [$c$] is the salt concentration in mole.$l^{-1}$ and, $E_0 \propto \sigma^2/c$, where $\sigma$ is the surface charge density.

Beside these « classical » forces, Helfrich has proposed a novel interaction arising from the steric hindrance of undulating neighbouring membranes. The entropy difference between a « free » and a « bound » undulating membrane in a multilamellar phase has been calculated by Helfrich [4] with use of the Landau-de Gennes [15, 17] elastic free energy per unit volume given by equation (1). This undulation induced interaction per unit surface is given by :

$$f_{und} = \frac{3\,\pi^2}{128} \frac{(kT)^2}{k_c} \frac{1}{d^2} . \quad (14)$$

Thus, *the Helfrich interaction is repulsive and very importantly long range.* Moreover, it is inversely proportional to the elastic bending modulus for a single membrane $k_c$.

In an earlier publication [1] we demonstrated that in suitable systems, the entropically induced interaction dominates. As we shall demonstrate, the two requirements necessary for this interaction to dominate are a small value of $k_c \approx k_B T$ (because the interaction is thermally induced) and the absence of a strong long range electrostatic force. In this paper, we elucidate the intermembrane interactions along both a water and a brine dilution path which corresponds respectively to systems which exhibit long and short range electrostatic forces. The comparison between undulation forces and electrostatic forces will then be possible.

## 4. Experimental systems.

The basic system studied is a ternary mixture of water, SDS (Sodium Dodecyl Sulfate) and pentanol. The phase diagram at room temperature and atmospheric pressure is shown figure 2a (from Ref. [25]). The detailed effect of temperature has been previously published [25]. Four different phases exist at room temperature. Phases E and R are respectively hexagonal and rectangular, phase L is an isotropic liquid phase and phase D is a lamellar phase.

The second system studied corresponds to one where the solvent (water) has been replaced by brine (≈ 0.5 M NaCl ). The phase diagram of this four component mixture should be represented as a tetrahedron (at constant pressure and temperature). We show in figure 2b a schematic cut (only the lamellar phase is represented) of this three dimensional phase diagram at a fixed salt over water ratio corresponding to the salt concentration used for the brine (0.5 mol.$l^{-1}$). This cut and other cuts of the same phase diagram have been mapped out in detailed by G. Guerin [26]. The main effect of the addition of a salt is to stabilize the lamellar phase over a much larger dilution range (from $d \approx 100$ Å without salt to $d > 500$ Å with 0.5 mol.$l^{-1}$ of NaCl).

For the X-ray experiments, we have prepared samples in the lamellar phase D (represented by dots in the Figs 2a and 2b). The samples were prepared by weighing the different constituents. After mixing, the samples are placed in sealed capillaries (diameter 1 mm).

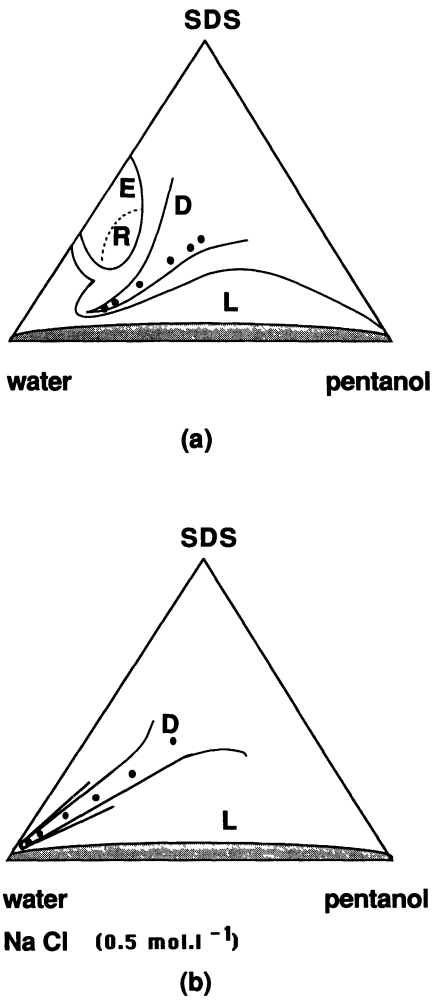


Fig. 2. — Phase diagrams of the two systems studied. The notation corresponds to different phases, E is hexagonal, R is rectangular, D is lamellar and L is a liquid isotropic phase. a) Corresponds to the phase diagram of the ternary mixture water, SDS and pentanol ($T$ = 24 °C, from Ref. [25]). The dots indicate the 6 mixtures studied. b) The phase diagram is only schematic and represents a cut for a salinity of 0.5 mol · $l^{-1}$ of the three-dimensional representation of the phase diagram of the quaternary mixture water, pentanol, SDS and salt. The dots indicate the 6 mixtures studied.

**5. Results and analysis.**

The samples prepared as described above consist of randomly oriented domains, the quality of the powder was checked by standard crystallographic scans ensuring that no partial orientation existed. We show in figure 3 a series of scattering profiles for longitudinal scans through the first harmonic along the water dilution path for the weight fraction of water ($\Phi_w$) increasing from 0.47 to 0.77. In figure 4 we plot scattering data along the brine dilution path with $\Phi_w$ increasing from 0.44 to 0.88. The first sample of the brine series and several samples of the water series exhibit both the first harmonic and second harmonics of the structure factor. (The second harmonic is not plotted in figures 3 and 4 ; figure 8 shows an example of the first and second harmonic.)

From the X-ray data we deduce the following. First, the first and second harmonics confirm the lamellar structure. In dilute samples where the second harmonic is absent the existence of focal conic defects confirms the smectic-A type structure. Second, the power-law line shape enables a meaningful thermodynamic analysis. We find that by adding water or brine we move along a true dilution keeping the membrane thickness constant as the mean separation is increased. This can be quantitatively checked if we assume that the density of all the constituents remains constant. Indeed, all the surfactant and the alcohol molecules are incorporated in building the membrane (the CMC of the SDS is much smaller than the concentration we used and pentanol is almost insoluble in water). From geometric considerations, we readily find that the repeat distance $d_u$ is predicted to be inversely proportional

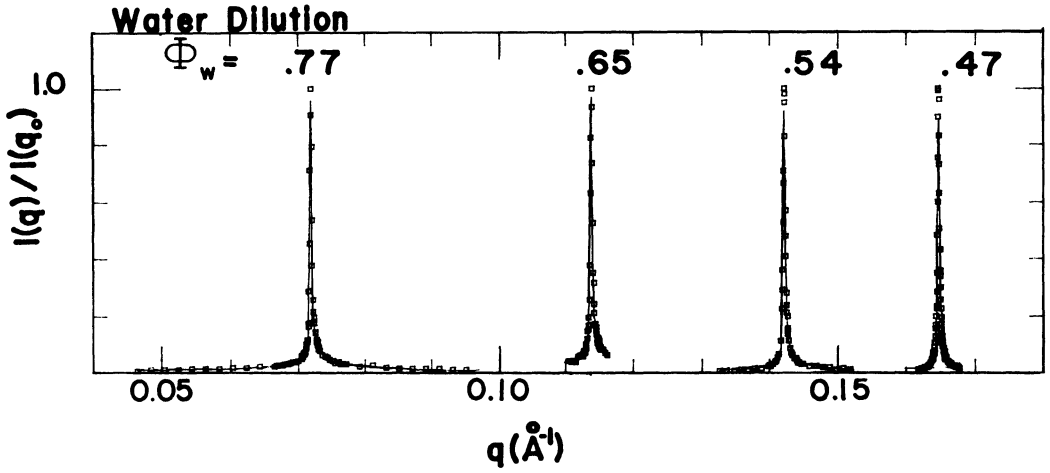


Fig. 3. — Longitudinal profiles of the first harmonic of four different mixtures along the water dilution path. The percentage water by weight of the mixture $\Phi_w$ is indicated above each profile. The solid lines are fits by the full Caillé expression given by equation 17 as discussed in the text. All peak intensities are normalized to unity.

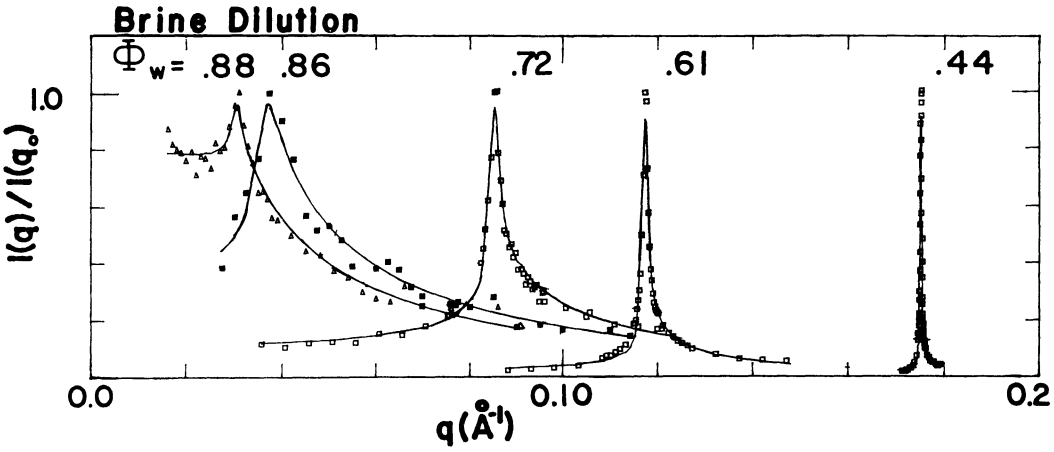


Fig. 4. — Longitudinal profiles of the first harmonic of five different mixtures along the brine dilution path. The percentage brine by weight of the mixtures $\Phi_w$ is indicated above each profile. The solid lines are fits by the full Caillé expression given by equation 17. All peak intensities are normalized to unity.

to the volume fraction of surfactant plus alcohol [27] :

$$d_u = \frac{\delta}{\Phi_s + \Phi_a} = \frac{\delta}{1 - \Phi_w^v}. \quad (15)$$

Figure 5 shows a plot $d_u$ for both the water and the brine dilution as a function of $1/(1 - \Phi_w^v)$, the anticipated linear behaviour is indeed observed and the thickness of the layer $\delta$ is found to be the same for both the water and brine dilution and equal to 20 Å. From the actual composition we calculate the area per amphiphile head which is found to be about 23 Å$^2$ per chain (SDS or pentanol assuming that they have the same area per head), this value which is close to the limiting value for chain packing (21 Å$^2$) indicates that the film is compact compared to a lamellar phase of pure surfactant where the area per polar head is around 35 Å$^2$ [28].

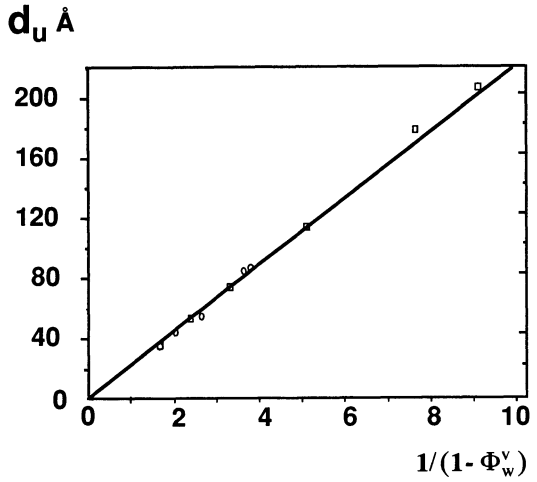


Fig. 5. — Plot of the repeat distance $d_u$ of the lamellar phase (measured by the peak position of the structure factor) as a function of $1/(1 - \Phi_w^v)$ for the two systems studied (circles : water dilution, squares : brine dilution). The linear function indicates a dilution of the lamellae corresponding to the conservation of the volumes (all the surfactant and practically all the alcohol molecules forms bilayers of thickness $\delta$ = 20 Å separated with pure water or pure brine).

A very important and striking feature of the profiles of the peaks shown in figure 4 is the tail scattering which becomes dramatically more pronounced as $d_u$ increases along the brine dilution path. This effect is due to the thermal fluctuations as explained in part 2 and which we will now elucidate in detail. This is in contrast to the scattering profiles observed along the water dilution path shown in figure 3. Qualitatively, in this latter case, the profiles are quite similar as $d_u$ increases although quantitative analysis reveals small differences as we shall discuss. We show in figure 6 on a semi-log scale the scattering

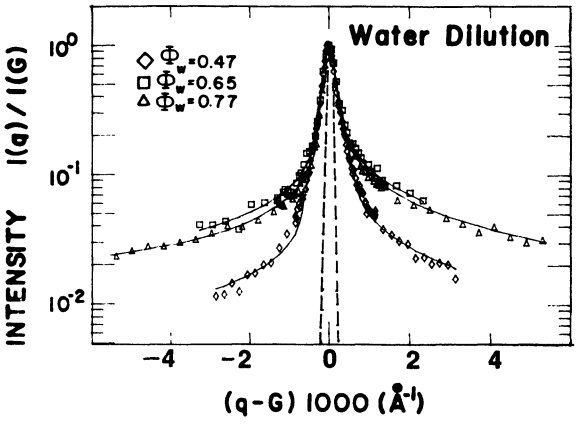


Fig. 6. — Profile of the first harmonic ($G = q_0$) for three mixtures along the water dilution path plotted on a logarithmic intensity scale. The solid lines are fits by the Caillé power-law line shape (Eq. 17). All peak intensities are normalized to unity.

profile for three samples of the water dilution series, $\Phi_w$ = 0.47, 0.65, 0.77. The difference in the profiles over the entire water dilution range is now clear. The exponent $\eta$ which characterizes the scattering profile is a direct measure of the tail to peak intensity ratio. We find that initially $\eta$ increases between $\Phi_w$ = 0.44 and $\Phi_w$ = 0.65 and levels off between $\Phi_w$ = 0.65 and $\Phi_w$ = 0.77 as elucidated in figure 6. This behaviour is very different from that observed for the brine dilution (Fig. 4) where the tail to peak intensity grows continuously indicating that $\eta$ increases along the dilution. We analyse the profiles quantitatively using the Caillé calculation [18]. Since we are dealing with an unoriented sample we cannot use the simple asymptotic expressions given by equations (2a) and (2b) but instead we fit our data with the Fourier transform of the correlation function given by equation (4). We now present details of the fitting procedure used.

The dashed lines in figure 6 show the longitudinal resolution function. The widths of the profiles are very close to the resolution for the water dilution but larger than resolution for the brine dilution, indicating that the domain size is smaller when salt is present. However, we stress that the typical domain sizes are unusually large between 2 000 Å and > 10 000 Å, which allowed for meaningful analysis of the profiles. We incorporate the finite size effect in our analysis in a straightforward manner outlined by Dutta and Sinha [29]. This then modifies the structure factor :

$$S_{FS}(\mathbf{q}) \propto \int d\mathbf{R}\, G(\mathbf{R})\, e^{-\pi \frac{R^2}{L^2}}\, e^{i(\mathbf{q} - q_m \hat{z}) \cdot \mathbf{R}} \quad (16)$$

where $L^3$ is the finite domain volume and $q_m = mq_0$. $G(\mathbf{R})$ is the correlation function and is given by equation (4). Finally, because the samples consist of

randomly oriented domains, we perform a powder average over all solid angles in reciprocal space. The finite size and powder averaged structure factor is given by :

$$S(q) = \langle S_{FS}(\mathbf{q}) \rangle \propto \int_{-\infty}^{+\infty} dz \int_{0}^{+\infty} dr\, G(z, r) \times \times e^{-\pi \frac{R^2}{L^2}} \frac{\sin(qR)}{qR} e^{-iq_m z} . \quad (17)$$

The analysis consists of a least squares fit of equation (17) convoluted with the resolution function (represented as Gaussian functions) to the experimental profiles. The solid lines in figures 3 through 7 are results of the best fits to the data with five fitting parameters : $I_m$ the intensity of the peak maximum, $\eta$, $\lambda$, $L$ and $q_m$. Figure 7 shows plots of the experimental and theoretical profiles for two samples, one along the brine dilution $\Phi_w = 0.72$, the other along the water dilution $\Phi_w = 0.77$ with approximately the same intermembrane spacing. The results plotted on a log-log scale elucidate the main features of the profiles. At large $q$ the profiles are linear indicating a power law decay of the scattering intensity as expected from Caillé's expression :

$$S(q) \propto |q - q_0|^{-p} , \quad \text{for} \quad |q - q_0| > 2\pi/L$$

the exponent $p$ is approximately equal to $1 - \eta$ due to the powder averaging [30]. For small $|q - q_0| < 2\pi/L$ the finite size effects dominate and round off the observed profile with a characteristic width equal to $1/L$. We point out the large difference in the slope for the two samples (Fig. 7) reflecting the more than a factor two difference in $\eta$ ($\eta = 0.71$ for the brine dilution ($\Phi_w = 0.72$) and $\eta = 0.31$ for the water dilution sample ($\Phi_w = 0.77$)). We see in figure 7, that for large $|q - q_0| > 10^{-2}$ Å$^{-1}$ the scattering deviates from the power law behaviour falling off faster. This is because the effect of the powder averaging is less important for $q$ very far from the sphere of scattering and in fact one expects a cross-over to the power law behaviour $S(q) \propto |q - q_0|^{-2+\eta}$ for scattering predicted by an oriented lamellar phase.

A further more subtle aspect of the data is shown in figure 6 where the profiles are slightly asymmetric with the high $q$ region more intense than the low $q$. This effect which is also seen in the theoretical fit is due to the parameter $\lambda = \sqrt{K/B}$ which enters in the real space correlation function $G(\rho, z)$ (Eq. (4)). This parameter is a measure of the anisotropy present in $S(q)$. This effect is only observable for $\lambda < 2\pi/q_0$ ; for larger values of $\lambda$ the asymmetry is negligible and $S(q)$ is not sensitive to the value of this parameter. In our case, $\lambda$ remains small enough to be measurable (except for the last sample of the brine dilution). The above analysis cannot be reasonably applied to cases where $\eta$ is extremely small ; for example, for $\eta < 0.01$. For $\eta = 0$, $S(q)$ as given by equation (17) reduces to :

$$S(q) \propto \frac{L}{qq_0} \left[ e^{-\frac{(q-q_0)^2 L^2}{4\pi}} + e^{-\frac{(q+q_0)^2 L^2}{4\pi}} \right] .$$

Thus, in this limit, $S(q)$ is dominated by the finite size effect and not by the algebraic decay of the spatial correlations. From equation (4) we also point

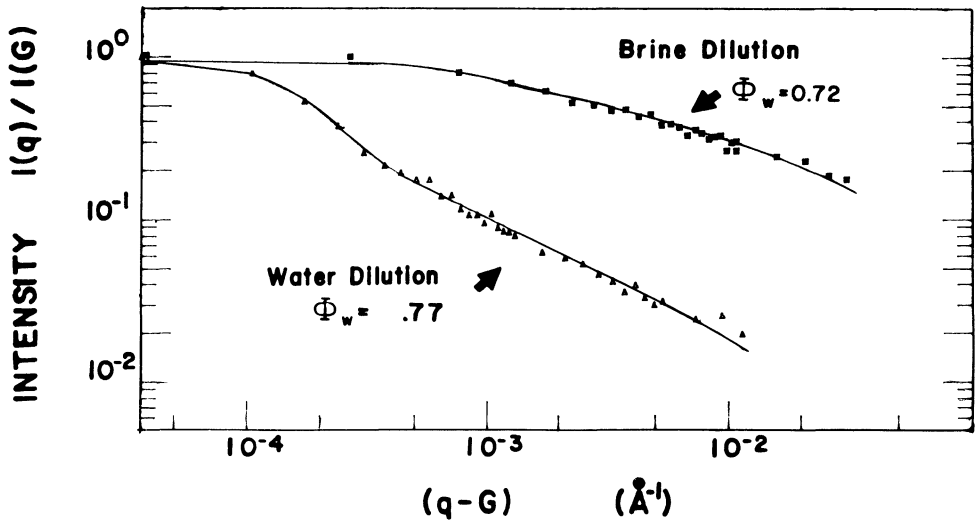


Fig. 7. — Profile of the first harmonic ($G = q_0$) for the mixture $\Phi_w = 0.72$ and $\Phi_w = 0.77$ along the brine dilution and water dilution paths respectively. The plots are on a log-log scale which shows finite size rounding at small $q$-$G$ as discussed in the text. The solid lines are fits by the full Caillé line shape (Eq. (17)). The figure shows the large difference in slope which is indicative of the difference in the interactions between membranes with similar interlamellar spacings but separated by different solvents (water or brine). All peak intensities are normalized to unity.

out that in the limit $\eta \to 0$, the dependence of $G(R)$ on $\lambda$ vanishes much more rapidly than its dependence on $\eta$.

The first sample of the brine dilution and several of the water dilution exhibit a second harmonic peak in addition to the first harmonic. This feature which is different from the regular thermotropic smectic A systems [19], allows us to self consistently verify the validity of Caillé's harmonic model. Indeed, as is evident from equation (3), $\eta$ scales with $m^2$ where $m$ is the harmonic number. The value of $\eta$ should be four times larger for the second harmonic than for the first harmonic. We show in figure 8 the profiles and the fits for the first and second harmonic for a sample along the water dilution $\Phi_w = 0.47$. The analysis involves a simultaneous fit to the first and second harmonic of the structure factor yielding $\eta_1 = 0.16 \pm 0.01$, $\lambda_1 = 6 \pm 2$ Å, $L_1 = 12\,500 \pm 1\,000$ Å and $\eta_2 = 4\,\eta_1$, $\lambda_2 = \lambda_1$, $L_2 = 10\,400 \pm 1\,500$ Å. This result indicates clearly that $\eta$ is effectively four times larger for the second harmonic while $\lambda$ and $L$ remain comparable. This also rules out the possibility that the broadening of the peaks with dilution would be due to intrinsic disorder, since in this case $L$ should scale with $m^2$ [31]. However, we point out that in some samples, the broadening parameter $L$ may be different by as much as 50 % between the first and the second harmonics. We do not completely understand all the possible origins of the peak width broadening but it is clear that the primary effect is due to a finite domain size.

To summarize the essential points in the fits, from the experimental data we are able to obtain four parameters : $q_0$, $\eta$, $L$ and $\lambda$ corresponding respectively to the peak position, the power law behaviour away from the central peak, the central peak width and the asymmetry in the profile around the peak. *What is spectacular is the observation of more than one order of magnitude increase in $\eta$ over the brine dilution range ;* this is a direct consequence of the large variation in the intermembrane interactions which we now discuss.

## 6. Interpretation and discussion.

The information we have on the thermodynamics of the system are contained in the shape of the peak. The value of $\eta$ is directly related to the interactions between the layers. Figure 9 shows the variation of $\eta$ as a function of $d_u$ for the water dilution and the brine dilution. In both cases $\eta$ increases as a function of $d_u$ but in a different way. For the water dilution $\eta$ saturates rapidly at a value around 0.3, while in the brine dilution $\eta$ continues to increase and saturates at a value larger than 1. This behaviour can be qualitatively interpreted as resulting from the damping of layer undulations in the water dilution compared to the brine dilution system. This is due to the existence of long range repulsive electrostatic interactions in the water dilution, as we will demonstrate in the following.

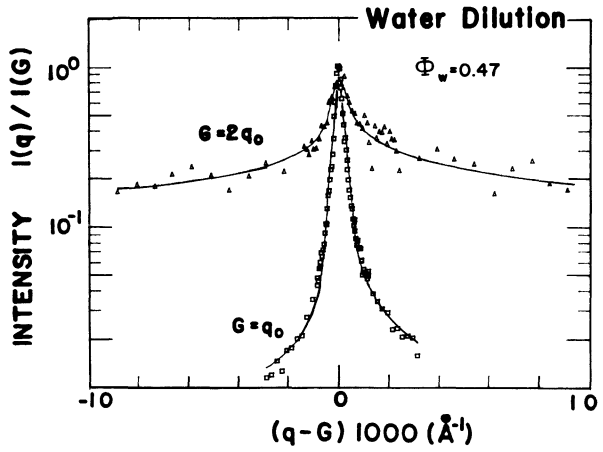


Fig. 8. — Profile for the first ($G = q_0$) and second ($G = 2\,q_0$) harmonics for the mixture $\Phi_w = 0.47$ along the water dilution path. The plot is on a logarithm scale. The large difference in the ratio of the peak to tail intensity is due to the scaling of the power law exponent $\eta_m$ with $m^2$ ($m$ = harmonic number) ; that is, $\eta_2 = 4\,\eta_1$. The solid lines represent a simultaneous fit by the Caillé line shape (Eq. 17) to both harmonics. Peak intensities have been normalized to unity for both harmonics.

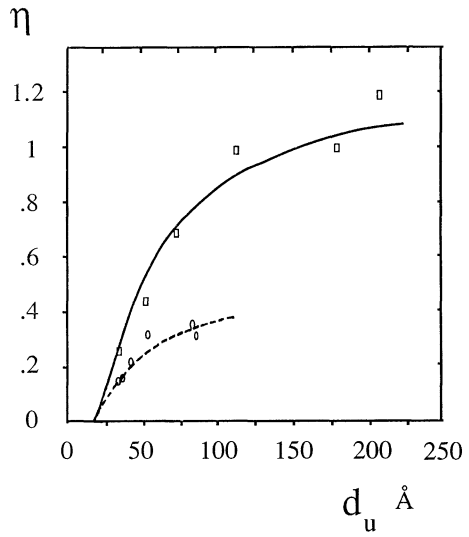


Fig. 9. — Variation of the exponent $\eta$ as a function of the repeat distance $d_u$ for the water dilution (open circles) and for the brine dilution (open square). The solid line corresponds to the prediction of the pure undulation interaction (Eq. 20), the dashed line is the solution of Poisson-Boltzman equation (Eq. 19). In each case, the values of all parameters are determined experimentally. $\delta = 20$ Å for both cases, for the water dilution : $k_c$ ranges from 2 $kT$ to 0.07 $kT$ and $\Sigma$ ranges from 80 to 190 Å$^2$).

From the free energy per unit surface, we readily calculate the layer compressional modulus $B$ and $\eta$ as a function of $d_u$. Indeed, $B$ is related to the second derivative of the free energy per unit volume :

$$B = d_u^2 \left[ \frac{\partial^2 \frac{F}{V}}{\partial d_u^2} \right]_n \quad \text{where} \quad \frac{F}{V} = nf \qquad (18)$$

where $n$ is the number of layers per unit length and $f$ the free energy per unit surface.

We perform the double derivative at constant number of layers using expressions given in part 3 and assuming that the thickness of the surfactant layers $\delta$ remain constant. In this manner we obtain an expression for $B$ as a function of $d_u$. The value of $\eta$ is then obtained using equation (3) together with $K = k_c/d_u$.

6.1 THE WATER DILUTION. — Since the electrostatic interaction are long range we expect this interaction to dominate for long distances, for short distances the hydration force can eventually dominate the electrostatic interaction [23] but all our experimental data are in a range where hydration forces can be neglected ($d > 15$ Å). Consequently, the simplest model we can use to understand the evolution of $\eta$ consists of taking the free energy per unit surface due to electrostatic forces given by equation (12). The calculation of $\eta$ as a function of $d$ is straightforward :

$$\eta = \left[ \frac{kTL_c}{2 k_c g} \right]^{1/2} \cdot \frac{[1 - \delta/d_u]^{3/2}}{d_u^{1/2}} \qquad (19)$$

with :

$$g = \left[ 1 - \frac{3 a_1}{d_u - \delta} + \frac{6 a_1^2}{(d_u - \delta)^2} \right] \quad \text{and} \quad a_1 = \frac{\Sigma}{\alpha L_c}.$$

Figure 9 shows the results of the comparison between the experimental and theoretical values of $\eta$ (open circles for the experimental data and dashed curve for the theoretical prediction). We set $\alpha = 1$ (assuming complete dissociation), $k_c$ is the value obtained from the measured values of $\lambda$ ($\sqrt{K/B}$) and $\eta$ ($\propto 1/\sqrt{KB}$) ($k_c$ varies smoothly from 2 $kT$ to 0.7 $kT$), and $\Sigma$ corresponds to the value calculated from the known composition of alcohol and surfactant ($\Sigma$ increases from 80 Å$^2$ to 190 Å$^2$ since for the water dilution (Fig. 2a) the alcohol over surfactant ratio varies continuously along the dilution), $\delta$ is 20 Å (resulting from the measured thickness of the surfactant layer (Fig. 5)). The good agreement indicates that a simple model of electrostatic interaction with no adjustable parameters is sufficient to interpret the experimental data. We find from numerical estimates (see Sect. 3) that both van der Waals and undulation forces are weak compared to the long range electrostatic forces. A full calculation of $\eta$ including these two other interactions does not significantly change the expected value of $\eta$ from the dashed curve shown in figure 9. We stress that these measurements are among the few cases where detailed predictions made by the simple one dimensional Poisson-Boltzmann equation have been quantitatively tested.

6.2 BRINE DILUTION. — In this case, the electrostatic interactions are short range with a screening length $\lambda_D \approx 6$ Å (0.5 M NaCl). We expect again that undulation forces will dominate (since $k_c \approx k_B T$) analogous to the behaviour found earlier [1] for the dodecane dilution. Therefore, for the brine dilution mixture the interlamellar forces must be dominated by entropic undulations [32]. We then expect $\eta$ to follow the Helfrich prediction given by equation (14) [1] :

$$\eta_{und} = \frac{4}{3} \left[ 1 - \frac{\delta}{d_u} \right]^2. \qquad (20)$$

The solid line in figure 9 is the predictions of $\eta_{und}$ with $\delta = 20$ Å (the same as the water dilution). The data (open squares) are the results of $\eta$ for the first harmonic in the brine dilution series. *Quite clearly, when only short range electrostatic forces are present, undulation forces dominate.*

6.3 DISCUSSION. — We combine the results of earlier work [1, 9] in presenting a broad picture of the interactions in model fluid membrane systems consisting of multilayer lamellar phases. In fluid multilamellar phases at finite temperature, thermal fluctuations of long-wavelength modes lead to a Landau-Peierls unstability that enables us to accurately measure a characteristic power law exponent $\eta \propto 1/\sqrt{KB}$ related to the inverse square root of the product of the bulk moduli for curvature ($K$) and compressional ($B$) for these systems. The layer compressibility modulus $B$ arises directly from the interactions between the membranes which occur on length scales smaller than the distance between the membranes.

In lipid-water systems with large membrane flexibility $k_c$ [9], interlayer interactions are dominated by the hydration force which is consistent with the earlier work of Parsegian *et al.* and Rand [3, 10]. Measurements of $k_c$ for these systems give values around $\approx 20\, k_B T$ [33] so that undulation forces are negligible. Thus, for these systems, long range attractive van der Waals forces overcome the repulsive short range force for intermembrane distances larger than 20 Å preventing any further solvent dilution. We have studied three other systems : (i) a previous dodecane dilution study (see Ref. [1]) on a multilayer system where the membrane is composed of a mixture of SDS, pentanol and water and (ii) the

present work on multilayer systems where the membrane is composed of a mixture of SDS and pentanol diluted with water or brine. In these systems, large dilutions up to several hundreds of angstroms is possible due to the existence of a long range repulsive interaction which overwhelms the only long range attractive interaction (van der Waals). When diluting the SDS-pentanol membrane system with pure water as we demonstrated, the compressional modulus $B$ arises primarily from long range repulsive electrostatic forces and entropic forces are negligible. In the absence of this electrostatic interaction, the undulation interaction dominates. Both dilutions with dodecane and with brine exhibit very similar behaviour ; the variation of the exponent $\eta$ (characterizing the algebraic decay of the structure factor) with the distance between layers follows a very simple expression predicted by the Helfrich theory [4]. An elegant way to show this behaviour is to plot the experimental value of $\eta$ as a function of $(1 - \delta/d_u)^2$ where $\delta$ and $d_u$ are experimentally measured. Indeed, the Helfrich theory predicts that $\eta = 1.33\ (1 - \delta/d_u)^2$.

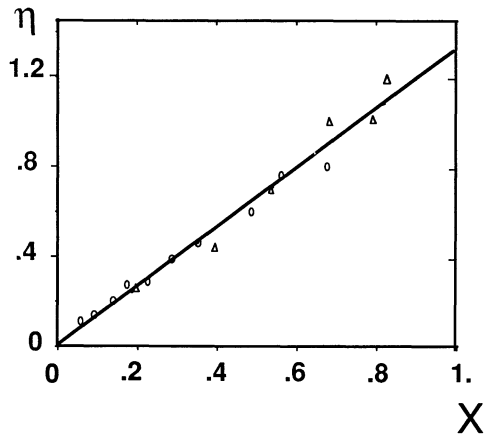


Fig. 10. — Plot of the value of the exponent $\eta$ *versus* the reduced distance squared $X = (1 - \delta/d_u)^2$ for the data where the undulation forces are dominant. The circles correspond to the dodecane dilution (see Ref. [1]) and the triangles corresponds to the brine dilution (this work). The straight line is the prediction of the Helfrich theory (Eq. (20)).

Figure 10 shows such a plot for the dodecane and brine dilution data where the undulation forces dominate. The straight line corresponds to a slope 1.33 as predicted by the theory. The agreement is remarkable indicating that not only is the $d$ dependence of the undulation forces correctly predicted by the Helfrich theory ($f \propto 1/d^2$) but also the multiplicative numerical factor. We emphasize, once again, that the comparison between experiment and theory is made without any adjustable parameter. Although at first, this rather excellent agreement between experiment and theory may come as a surprise, we point out that because the measured inter-membrane interactions are occurring at length scales large compared to microscopic lengths, continuum statistical mechanical considerations used in the Helfrich model should be valid.

## 7. Conclusion.

Using the property that the marginal dimension for the lyotropic lamellar $L_\alpha$ phase is three, that is, that long wave length layer fluctuations diverge as the logarithm of the sample size, we have shown that it is possible to measure from the X-ray structure factor the exponent $\eta(d)$ which characterizes the algebraic decay of layer correlations, and which in turn enables a direct measurement of the intermembrane interactions. We have demonstrated that aside from the « classical » forces characterized in the last 20 years (hydration, van der Waals and electrostatic) another interaction theoretically proposed by Helfrich [4] may dominate under suitable conditions. This entropically induced interaction originates from the steric hindrance of the thermal undulations of the membrane bound between two neighbours. This undulation interaction is shown to dominate in the absence of long range electrostatic interactions when the elastic modulus for bending the membrane is small (such as in a film composed of a mixture of surfactant and short chain alcohol molecules). The behaviour of this interaction is predicted quantitatively by the Helfrich theory. When strong long range electrostatic interactions exist, even if long wave length fluctuations remain present (Landau-Peierls effect), short wave length fluctuations are suppressed and the interaction between lamellae is dominated by electrostatic forces. A similar effect has been observed recently in another system [36]. Several questions regarding the ability to control this interaction are not yet clear and remain to be answered. For example, a small value of $k_c$ seems to be intimately connected to the fact that the film is composed of a mixture of surfactant and alcohol and although several authors have attempted to understand the role of the alcohol [12, 34], the role of the cosurfactant remains unclear. Another and even more important challenge is the relevance of the undulation interaction for real cell membrane system [35].

The authors would like to acknowledge A. M. Bellocq and G. Guerin for the phase diagrams and D. Andelman, P. Chaikin, S. Grüner, S. Leibler, V. Luzzati, R. Lipowsky, S. Milner, P. Pershan and S. Safran for discussions. One of us (D.R.) is grateful to W. G. Gelbart for his kind hospitality and stimulating discussions. It is a particular pleasure to acknowledge assistance from the Exxon staff mem-

bers at the Exxon beam line, especially R. Hewitt and M. Sansone. Finally we are grateful for technical assistance and stimulating scientific discussions with G. S. Smith and E. B. Sirota. The National Synchrotron Light Source at Brookhaven National Laboratories is supported by the U.S. department of energy.

## References

[1] SAFINYA, C. R., ROUX, D., SMITH, G. S., SINHA, S. K., DIMON, P., CLARK, N. A. and BELLOCQ, A. M., *Phys. Rev. Lett.* **57** (1986) 2718.

[2] ISRAELACHVILI, J. N., *Intermolecular and surface forces* (Academic Press, Orlando) 1985.

[3] PARSEGIAN, A., FULLER, N. and RAND, R. P., *Proc. Natl. Acad. Sci.* **76** (1979) 2750.

[4] HELFRICH, W., *Z. Naturforsch.* **33a** (1978) 305.

[5] LIPOWSKY, R. and LEIBLER, S., *Phys. Rev. Lett.* **56** (1986) 2561.

[6] DE GENNES, P. G., *Scaling Concepts in Polymer Physics* (Cornell Univ. Press) 1979.

[7] MOCHRIE, S. G. J. KORTAN, A. R., BIRGENEAU, R. J. and HORN, P. M., *Z. Phys. B* **62** (1985) 79.

[8] HELFRICH, W., *J. Phys. France* **46** (1985) 1263 ; PELITI, L. and LEIBLER, S., *Phys. Rev. Lett.* **54** (1985) 1690.

[9] SMITH, G. S., SAFINYA, C. R., ROUX, D. and CLARK, N., *Mol. Cryst. Liq. Cryst.* **144** (1987) 235.

[10] RAND, R. P., *Ann. Rev. Biophys. Bioeng.* **10** (1981) 277.

[11] LARCHÉ, F., APPELL, J., PORTE, G., BASSEREAU, P. and MARIGNAN, J., *Phys. Rev. Lett.* **56** (1986) 1700.

[12] DIMEGLIO, J. M., DVOLAITSKY, M. and TAUPIN, C., *J. Phys. Chem.* **89** (1985) 871.

[13] DIMEGLIO, J. M., DVOLAITZKY, M., LEGER, L. and TAUPIN, C., *Phys. Rev. Lett.* **54** (1985) 1686.

[14] DE GENNES, P. G. and TAUPIN, C., *J. Phys. Chem.* **86** (1982) 2294.

[15] a) LANDAU, L. D., in collected papers, edited by D. Ter Haar (Gordon and Breach, New York) 1965, p. 209.
b) PIEIERLS, R. E., *Helv. Phys. Acta* **7** (1974) suppl. 11, 81.

[16] DUTTA, P., SINHA, S. K., VORA, P., PASSEL, L. and BRETZ, M., *Ordering in two dimensions,* S. K. Sinha editor (Elsevier North Holland, Inc.) p. 169 ; HEINEY, P., STEPHENS, P. N., BIRGENEAU, R. J., HORN, P. M. and MONCTON, D. E., *Phys. Rev. B* **28** (1983) 6416.

[17] DE GENNES, P. G., *The Physic of Liquid Crystals* (Clarendon Oxford) 1974.

[18] CAILLÉ, A., *C.R. Hebd. Séan. Acad. Scien. Ser. B* **274** (1972) 891.

[19] ALS-NIELSEN, J., LITSTER, J. D., BIRGENEAU, R. J., KAPLAN, M., SAFINYA, C. R., LINDEGAARD-ANDERSEN and MATHIESEN, S., *Phys. Rev. B.* **22** (1980) 312.

[20] BONSE, U. and HART, M., in *Small Angle X-ray Scattering,* edited by H. Brumbeger (N.Y. Gordon & Breach).

[21] MAHANTY, J. and NINHAM, B. W., *Dispersion Forces* (London) 1976.

[22] MARRA, J., *J. Coll. Int. Sci.* **109** (1986) 11.

[23] COWLEY, A. C., FULLER, N. L., RAND, R. P. and PARSEGIAN, V. A., *Biochem.* **17** (1978) 3163.

[24] LEIBLER, S. and LIPOWSKY, R., *Phys. Rev. B* **35** (1987) 7004.

[25] BELLOCQ, A. M. and ROUX, D., *Microemulsion,* Frieberg, and Bothorel, P. editors.

[26] GUERIN, G., Thesis (Bordeaux 1986).

[27] LARCHE, F. C., MARIGNAN, J. and EL QEBBAJ, S., *J. Phys. Chem.* **90** (1986) 707.

[28] LUZZATI, V., MUSTACHI and SKOULIOS, *Disc. Faraday Soc.* **25** (1958) 43.

[29] DUTTA, P. and SINHA, S. K., *Phys. Rev. Lett.* **47** (1981) 50.

[30] Indeed, the powder averaging is a surface integral which reduces the power of the effective Caillé exponent by 2. The effective Caillé exponent after powder averaging can be crudely estimated by the mean average of the asymptotic power laws of equation (6) : $(2 - \eta)/3 + 2(4 - 2\eta)/3 = (4 - 5\eta)/3$. The simple behaviour for $p \sim 1 - \eta$ is approximatively accurate only when $\sigma_q/q_0 < 0.01$, which is the case for the samples studied in this paper. $\sigma_q$ is the root-mean-square of $S(q)$ and is related to the finite domain size $L = \sqrt{2\pi}/\sigma_q$ (see Eq. (16)).

[31] GUINIER, A., X-ray Diffraction (W. H. Freeman and Co) 1963.

[32] In fact hydration forces, may be expected to be important only for the least dilute mixture where $d \approx 16$ Å.

[33] SCHNEIDER, M. B., JENKINS, J. T. and WEBB, W. W., *J. Phys. France* **45** (1984) 1457.

[34] LEIBLER, S., *J. Phys. France* **47** (1986) 507.

[35] HELFRICH, W. and SERVUSS, R. M., *Il Nuovo Cimento* **3** (1984) 137.

[36] BASSEREAU, P., MARIGNAN, J., PORTE, G., *J. Phys. France* **48** (1987) 673.